

# Comparison of Wireless Data Transmission Protocols for Residential Water Meter Applications

Łukasz Krzak, Jan Macheta, Mateusz Kubaszek, and Cezary Worek

**Abstract**—This article provides a comparison of various wireless data transmission protocols, such as Wireless M-Bus, LoRaWAN, Sigfox, NB-IoT and a newly developed proprietary protocol, studying their performance in the application of battery-powered residential water meters. Key aspects of the comparison include energy consumption, which is analyzed through comparing unitary amount of charge required to conduct a single, bidirectional data transaction between the meter and base station, and maximum coupling loss which effectively defines the range and coverage in the system. For completeness, the study includes also a brief cost analysis and ends with a conclusion, stating when each of the particular standards should be favored.

**Keywords**—Water meter; protocol; Wireless M-Bus; LoRaWAN; Sigfox; NB-IoT; energy consumption; maximum coupling loss

## I. INTRODUCTION

MODERN society places increasing demands on municipal infrastructure and effective management of water resources plays a key role in meeting these needs. Water meters, which are a basic tool for monitoring and recording water consumption by households, enterprises and other entities, have undergone a long way of evolution, adapting to the growing market needs and technological progress. One of the important aspects of these changes, which significantly influences the way of constructing, implementing and using water consumption settlement systems, is the data transmission technology used. Today it is largely wireless, based on various radio communication protocols and standards.

The aim of this article is to review and compare different techniques and standards that are used in the application of remote communication with water meters in terms of key technical features that determine important operational parameters, such as battery lifetime, range and coverage, required telecommunications infrastructure, as well as the cost of implementation. This work is also a result of collaboration between the Authors and a water metering company Actislink, that led to the development of a new proprietary wireless communication protocol, which we also include in the comparison.

The article presents the results of R&D work carried out as part of the project entitled "Development of a dual-band LPWAN network dedicated to work in utility consumption metering systems", co-financed by the European Union under sub-measure 1.2.1 "Research and development projects of enterprises", Regional Operational Programme for the Małopolska Region 2014-2020.

Ł. Krzak, J. Macheta, M. Kubaszek and C. Worek are with Institute of Electronics, Faculty of Computer Science, Electronics and Telecommunications, AGH University of Krakow, Krakow, Poland (e-mail: lkrzak@agh.edu.pl).

In this paper we thus give the motivation behind that work and compare the results with other popular solutions. It is worth highlighting that the source code of the models and tools used to create this comparison is available online in the repository provided by the Authors [1].

The rest of the paper is organized in the following way. Chapter II includes historical context and shares information about current water meter market, Chapter III describes related work, Chapter IV discusses the challenges and requirements for the communication protocols and Chapter V gives brief introduction to the analyzed protocols and standards. Next, Chapters VI, VII and VIII provide detailed analysis of energy consumption, link budget and cost respectively, while Chapter IX gives the conclusions.

## II. HISTORICAL CONTEXT

It isn't easy to pinpoint precisely where and when the first water meters with wireless communication were used, as the development of this technology was gradual and took place in different regions of the world almost simultaneously. The first water meters with remote reading began to appear between 1980 and 1990, and the technology was gaining popularity because it allowed water and sewage companies to automatically collect water consumption data without needing physical access to each meter. Wired technologies were used first [2], but were later replaced by wireless for convenience, as the digital radio transmission techniques and tools evolved [2]. In many developed countries, such as the United States, Canada, and Western European countries, water meters with wireless communication became a standard by the end of the 20th century.

Remote reading technology was deployed in water meters gradually, often as an extension, in the form of a separate overlay on a mechanical water meter. Such device is detecting the rotation of the element on the meter dial using optical or electromagnetic methods or (less frequently) by receiving pulses generated by the meter. For the past 10 years, integrated solutions, which often use ultrasonic measurement of the water flow, have become increasingly popular [3]. At the same time we have seen the slow decline of meters implemented with AMR (Automated Meter Reading) technology, which only allows one-way remote reading of water consumption, in favor of AMI (Advanced Metering Infrastructure) technology. Due to technical and business considerations, the former was usually operated in a walk-by (or drive-by) fashion, in which



a collecting person equipped with a suitable receiver had to periodically visit water meter sites and thus collect the data necessary to create billing. AMI water meters are a natural evolution of AMR technology, offering not only remote data reading, but also two-way communication between the meter and the central management system, based on a stationary communication infrastructure. This makes it possible to monitor water consumption in real time and identify and respond to leaks, failures, or unusual consumption patterns, sometimes indicative of fraud attempts.

The largest water meter market is North America, with about 82.8 million installed as of the end of 2021, of which about 34 million are classified as AMI meters. The second largest market is Europe, with about 62.9 million water meters, of which about 15.6 million are classified as AMI meters. In doing so, AMI technologies are projected to be deployed much more frequently than AMR in the next five years [4].

As for the communication techniques and standards used, they are also strongly region-specific [4]. In North America, proprietary solutions dominate, accounting for about 94% of all deployments, mainly based on data transmission in the unlicensed ISM (Industrial, Scientific and Medical) band from 902 MHz to 928 MHz. In Europe, the situation is somewhat more diverse. By 2022, nearly half of deployments used the Wireless M-Bus standard (EN 13757) operating mainly in the 868 MHz band, less frequently in the 169 MHz band. Other popular technologies include use of cellular infrastructure for data transmission, with the LTE-M and NB-IoT standards, as well as solutions based on Low Power Wide Area Networks (LPWAN) such as LoRaWAN and Sigfox, operating in the 863 to 870 MHz band.

### III. RELATED WORK

Although there are many publications analyzing and comparing various communication protocols for the Internet of Things (IoT) and smart metering applications [5], [6], not many focus on specific perspective of the water metering systems. Lale et al. [7] gives a good overview of the requirements and technologies but without going too deep into important details. Sushma et al. [8] gives an introduction to various aspects of the overall design of the water metering system, including the meter itself. Ruckebusch et al. [9] presents a very detailed energy consumption modeling with the goal to analyze the impact of over-the-air software updates in LPWAN networks on the battery lifetime. Various authors also present the design of the water meter which includes application of the wireless communication protocol [10], [11]. Finally, there are many publications analyzing in detail all the above mentioned protocols, including Wireless M-Bus [12], [13], LoRaWAN [14]–[16], Sigfox [17], [18] and NB-IoT [19]–[22].

### IV. CHALLENGES

The implementation of AMI-type remote communication with a water meter in residential buildings involves a number of difficult technical challenges. They often result from specific product requirements, which originate from the features that systems of this type had in the past. The most important of them will be described below.

#### A. Cost sensitivity

A water meter for residential buildings is an extremely price sensitive mass product. The high supply and competition in the market for this type of devices, as well as the price benchmark established by previous generation devices (AMR), make it very difficult to justify any additional costs in the production and deployment of these devices. It is also difficult to pass them on to the end users, who most often expect only minimal functionality, consisting in the settlement of water consumption. This means that the design of the electronic part of the water meter (responsible for communication) is strongly cost-optimized. This is evident in the offer of suppliers of components, e.g. microcontroller chips integrated with a radio transceiver, in which a separate category are systems dedicated to smart metering. Their aim is to offer minimal features (computing power, amount of FLASH and RAM memory, number of peripheral systems) for the most favorable price possible. Unfortunately, this leads to numerous technical compromises that the designers of these devices have to make, which have a strong impact on the possibilities of implementing various data transmission techniques.

#### B. Battery lifetime

In the case of residential buildings, the water meter is expected to be a battery-powered device, with a minimum battery life of 5 years plus additional one year of storage, sometimes reaching even up to 11 years. This is a direct result of the fact that in many European countries (including Poland) legalization of the water meter, which is a natural opportunity to replace it with a new one or replace the battery in it, takes place every 5 to 8 years, depending on the region and type of meter. At the same time, the dimensions and design of the water meter (or an electronic part of the meter supplied in the form of a separate overlay) impose significant limitations on the size, and thus the capacity, of the battery cell used to power both the reading and communication parts of the device. This, coupled with the aforementioned price sensitivity, results in the limited amount of available energy and greatly affects how remote communication with the water meter is implemented. Table I gives examples of battery types used in water meters.

TABLE I  
EXEMPLARY BATTERY CELLS USED IN WATER METERS

Producer	Model	Size	Capacity
Tadiran	SL-850	1/2 AA	900 mAh
Tadiran	SL-861	2/3 AA	1200 mAh
Tadiran	SL-860	AA	1800 mAh
Saft	LS14250	1/2 AA	800 mAh
Saft	LS14500	AA	1900 mAh

#### C. Communication range and coverage

Despite limitations related to the price and quality of components, as well as available energy, the effective communication range between the water meter and the collector's

receiver (in the case of a walk-by or drive-by systems) must be sufficient to carry out the data collection process in an uninterrupted manner, i.e., avoiding the need to get too close, or enter the premises where the meter is installed. In dense residential areas this challenge is further made more difficult by the location of the meters, which in older buildings are installed in various hard-to-reach places, often unfavorable for radio wave propagation. In the case of stationary AMI systems, the situation is even more difficult, as due to cost constraints, the aim is to maximize the number of water meters per single base station, which increases the requirements for capacity and reliability of the radio connection. In suburban areas on the other hand, the challenge is the area that needs to be covered. One favorable solution used by Wireless M-Bus in Europe to address this is using 868 MHz band in urban areas and 169 MHz in suburban areas.

## V. PROTOCOLS AND STANDARDS

### A. Wireless M-Bus

Wireless Meter-Bus is a European standard (EN 13757-4) primarily designed for reading utility meters. It predominantly operates in the 868-870 MHz band in Europe using Frequency-Shift Keying (FSK) modulation, but can also work in the 169 MHz and 433 MHz bands. The standard defines several communication modes [23]:

- **S** (Stationary): intended for stationary meters, uses 868 MHz band.
- **T** (Frequent Transmit): designed for battery-operated meters with frequent transmissions, uses 868 MHz band.
- **R** (Frequent Receive): Mostly for concentrators or data collectors, uses 868 MHz band.
- **C** (Compact): Offers slightly larger data rate to save energy, uses 868 MHz band.
- **N** (Narrowband): Offers long range operation in 169 MHz band.
- **F** (Frequent receive and transmit mode): Operates in 433 MHz band.

The standard supports AES-128 encryption and is often used together with the Open Metering System (OMS) specification in the application layer, to ensure interoperability. While the protocol defines also relay nodes, it is mostly deployed in a star topology, where distributed meters communicate directly with a base station or a mobile data collector. The protocol itself is fairly simple which translates to low memory footprint and low CPU usage. Also, since FSK modulation is available in many low-complexity radio transceivers, the hardware required to support Wireless M-Bus can be really low-cost [11].

### B. LoRaWAN

LoRaWAN (Long Range Wide Area Network) is a popular LPWAN (Low Power WAN) protocol designed for wireless battery-powered devices, operating predominantly in sub-GHz bands: 868 MHz (Europe) and 915 MHz (North America). It uses the LoRa modulation, which is based on chirp spread spectrum technique. LoRaWAN defines three classes of operation which dictate how the devices send and receive data:

- **Class A:** The mandatory and most energy-efficient class. Each uplink transmission is followed by two short downlink receive windows.
- **Class B:** In addition to the Class A operations, it opens extra receive windows at scheduled times, allowing for more downlink opportunities.
- **Class C:** Devices in this class have nearly continuous receive windows. This offers the maximum downlink availability but is much less power efficient.

LoRaWAN spread spectrum modulation allows to dynamically adapt the spreading factor (SF) and coding rate (CR) to a changing radio propagation conditions, which leads to an adaptive data rate (ADR) algorithm. In Europe, a LoRaWAN compliant device must support at least data rates marked DR0 to DR5, using channel bandwidth (BW) of 125kHz according to Table II.

TABLE II  
LoRaWAN DATA RATES IN EUROPE [24]

Data rate	SF	Bit rate (bit/s)	Max. payload (B)
DR0	12	250	51
DR1	11	440	51
DR2	10	980	51
DR3	9	1760	115
DR4	8	3125	242
DR5	7	5470	242

### C. Sigfox

Sigfox is another LPWAN protocol designed for long-range communication and low power consumption. Unlike Wireless M-Bus and LoRaWAN, which rely on user-deployed infrastructure, Sigfox operates as a global network operator and provider. The standard employs ultra-narrow band (UNB) modulation and operates in the 868 MHz band (in Europe) and the 915 MHz band (in North America).

Primarily optimized for uplink communication (device-to-cloud) with limited downlink capabilities, Sigfox imposes restrictions on data rates (100 bps or 600 bps, depending on the region). The maximum payload size for uplink messages is 12 bytes (8 bytes for downlink). Due to radio band occupancy restrictions, each device can transmit up to 140 uplink messages per day and is guaranteed to receive at least four downlink messages, with the potential for more if network resources are available [25]. The process of receiving downlink messages is initiated by the device: when sending an uplink message, the device may request the reception of a downlink message, and it then opens a reception window (max 25 seconds). If the base station has a message for the device, it is transmitted, and the device sends a downlink confirmation [26].

### D. NB-IoT

NB-IoT (LTE Cat NB1 and LTE Cat NB2) was designed as an addition to the existing LTE standard, to address the needs of the emerging IoT applications. It reuses many features of LTE and allows for easy deployment over existing cellular

network infrastructure, maintaining interoperability between the two. The protocol is far more complex than the aforementioned standards. At PHY and MAC level it features various mechanisms such as dynamic allocation of resources, adaptive modulation and coding scheme, configurable number of repetitions, variable output power and other to adapt the transmission scheme to radio propagation conditions. Similar to LoRaWAN, it thus allows to exchange energy spent on data transmission for range and better quality of service (QoS). When interacting with the NB-IoT network the device can either be in the CONNECTED or IDLE state. When connected, it can transmit and receive application data and can be considered reachable, with minimum delay. Battery-powered devices spend most of their operating time in IDLE state, as the CONNECTED state yields relatively high power consumption. By default the IDLE state requires the device to periodically poll the base station, signaling readiness to receive data. Devices targeting long battery life have basically two options when it comes to interacting with the NB-IoT network in IDLE mode. They can either use Extended Discontinuous Reception (eDRX) mode or Power Saving Mode (PSM). eDRX allows the device to significantly extend the periods between polling, thus reducing energy usage. But it is the PSM mode that actually makes the device run for years on battery, as it allows to enter deep sleep modes for longer periods of time (e.g. hours). It is however important to note, that several settings affecting polling intervals and thus energy consumption are controlled by the network operator and may be specific to a given installation.

### E. Mesh networks

In many applications mesh networks provide an important advantage over star-topology solutions, by introducing routing devices that have the capability to relay packets. This capability can significantly extend the coverage of the communication system, extending the connectivity to reach areas with worse propagation conditions, such as basements or remote locations. However, this advantage comes at a significant cost, which includes increased network complexity and higher energy consumption, as in most cases the routing devices are required to continuously listen for incoming transmissions. Another factor to consider is that most mesh network standards are designed to operate in the 2.4 GHz band, which has worse propagation properties than sub-GHz solutions. Due to these constraints in this article we will not consider mesh networks as a viable option for battery-powered water meters. We will only indicate below two possible approaches to mitigate the higher energy consumption problem, based on the nature of the mesh network.

1) *Heterogeneous Mesh Networks*: In heterogeneous networks, we explicitly distinguish routing devices from edge devices. This distinction is evident in LRWPAN protocols based on the IEEE 802.15.4 specification, such as Zigbee and Thread, as well as in Bluetooth Mesh. Due to the significant disparity in energy consumption, routing nodes are often mains-powered, which in residential water metering applications makes them a part of the data collecting infrastructure. With such infrastructure the water meters can act

as edge devices, and in that mode meet the battery lifetime requirements.

2) *Synchronized Mesh Networks*: Another possibility involves using a synchronized mesh network, such as 6TSCH [27]. In such networks all devices share a common time schedule and communicate in agreed-upon time slots and frequency channels. This allows for data transmission with minimal radio circuit activity and enables a low-power sleep mode when time slots are unoccupied. Detailed energy analysis for a 6TSCH-based solution can be found in [28]. Unfortunately, this solution has its drawbacks, including the initial energy consumption during network formation and the risk of network device battery depletion if the root device, on which the network relies, fails. One must also consider the disproportion of energy consumption between devices closer to the root, which statistically need to forward more traffic. On top of that optimizing the TSCH (Time-Slotted Channel Hopping) protocol operation involves selecting the appropriate PHY layer, MAC configuration (superframe and slot lengths), slot scheduler algorithm and routing protocol enhancements [29], [30] which makes this a complex task.

### F. Actislink - custom protocol for water meters

When designing a new, custom wireless communication system (named Actislink) for water meters we have defined the following important requirements:

- It should allow to reuse existing Wireless-MBus based hardware in water meters, or require just small adjustments, without affecting the price of components.
- It should support adaptive data rate, to allow link budget adjustment to radio propagation conditions.
- It should operate in two unlicensed radio bands: 868 MHz to deliver required capacity in urban areas and 169 MHz to extend coverage in suburban areas.

TABLE III  
PHY LAYER PARAMETERS IN THE ACTISLINK SYSTEM [31]

PHY no	Band	Direction	Number of channels	Bit rate [bit/s]
0	868 MHz	uplink	4	50000
1	868 MHz	uplink	2	1200
2	868 MHz	downlink	4	19200
3	868 MHz	downlink	4	19200
4	169 MHz	uplink	4	19200
5	169 MHz	uplink	4	9600
6	169 MHz	uplink	4	500
7	169 MHz	downlink	4	19200
8	169 MHz	downlink	4	9600
9	169 MHz	downlink	4	500

The base station was built using Software-Defined Radio (SDR) architecture [32] and it allows to receive incoming signals from water meters in parallel in all defined physical layers and radio channels (see Table III). Thus, the meters can operate in an opportunistic multiple access mode, transmitting at any time and selecting any (random) channel. The physical

layer is selected independently by each meter, based on the feedback (confirmations) sent back by the base stations. These confirmations can be received in a configurable number of reception (RX) slots, following uplink transmission (default: 3), as shown in Fig 1. Once confirmation is received in one of the slots, the other slots are canceled and the meter goes back to deep sleep mode immediately.

The base station calculates the path loss based on the received power level of the uplink transmission and sends it back to the meter with each confirmation. Based on this information the meter adapts the PHY used for the next transmission. The base station responds using a PHY based on the PHY number that was used for uplink transmission in the following way:

- if PHY 0 was used for uplink the confirmation is sent using PHY 2 (mode 0/2)
- if PHY 1 was used for uplink the confirmation is sent using PHY 3 (mode 1/3)
- if PHY 4 was used for uplink the confirmation is sent using PHY 7 (mode 4/7)
- if PHY 5 was used for uplink the confirmation is sent using PHY 8 (mode 5/8)
- if PHY 6 was used for uplink the confirmation is sent using PHY 9 (mode 6/9)

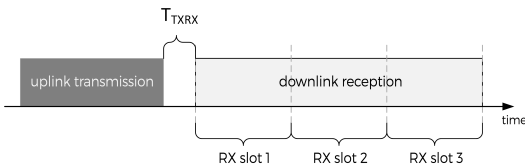


Fig. 1. Illustration of a single transaction in the Actislink protocol

VI. ANALYSIS OF ENERGY CONSUMPTION

In order to compare the impact of the chosen protocol on the energy consumption we will first model current consumption profiles for single data transaction between a water meter and data collector or base station as a step function. To make the comparison as fair as possible, we will assume the following:

- We only compare two-directional modes of operation of each protocol, even if the protocol features unidirectional mode with lower power consumption.
- Where possible, the uplink and downlink payload is always 16 bytes (with the exception of 12 for Sigfox), which corresponds to the standard AES-128 ciphering chunk size.
- In case there are multiple receive windows after the uplink transmission, we assume that the downlink reply comes in the first one (best case).
- When giving values of current we will assume operating voltage of 3.3 V, even if some transceivers can operate at lower voltage.

A. Wireless M-Bus transaction

For Wireless M-Bus we will consider modes S2, T2 and N2a. Fig. 2 presents the current consumption profile of a single

Wireless M-Bus transaction (here in S2 mode). The transaction is modeled for all modes as several steps, each described in Table IV [13].

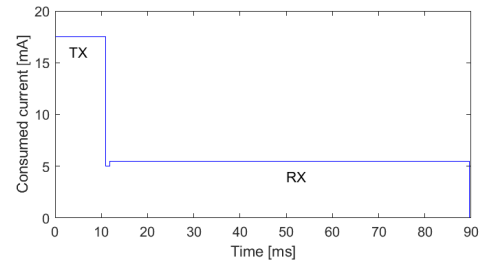


Fig. 2. Current consumption profile for a single Wireless M-Bus transaction. TX - data transmission state, RX - data reception state.

TABLE IV  
DESCRIPTION OF STEPS IN THE CURRENT CONSUMPTION PROFILE FOR WIRELESS M-BUS [33]

Step	Time [ms]	Current [mA]
Wake up	1.7	5
Packet transmission	$T_{TX}$	17.5
Switch from TX to RX	1	5.1
Packet reception	$T_{RX}$	5.5
RX switch off	0.3	5.1

Given parameters described in Table V the packet transmission time  $T_{TX}^{mode}$  can be expressed as [12]:

$$T_{TX}^{mode} = \frac{L_{preamble} + 2 + L_{up}}{R_{up}^{mode}} \tag{1}$$

and the packet reception time  $T_{RX}^{mode}$  as:

$$T_{RX}^{mode} = \frac{L_{preamble} + 2 + L_{ack}}{R_{down}^{mode}} \tag{2}$$

TABLE V  
WIRELESS M-BUS RELATED PARAMETERS FOR MODES S2 AND T2

Parameter	Symbol	Value
Uplink bitrate in S2 mode	$R_{up}^{S2}$	16384 bit/s
Downlink bitrate in S2 mode	$R_{down}^{S2}$	16384 bit/s
Uplink bitrate in T2 mode	$R_{up}^{T2}$	66666 bit/s
Downlink bitrate in T2 mode	$R_{down}^{T2}$	16384 bit/s
Uplink bitrate in N2 mode	$R_{up}^{N2a}$	4800 bit/s
Downlink bitrate in N2 mode	$R_{down}^{N2a}$	4800 bit/s
Preamble length	$L_{preamble}$	48 bits
Uplink payload size	$L_{up}$	128 bits
Ack payload size	$L_{ack}$	128 bits
Guard time	$T_{guard}$	30 ms

B. LoRaWAN transaction

For LoRaWAN will consider modes DR0 to DR5 according to Table II. Fig. 3 presents the current consumption profile

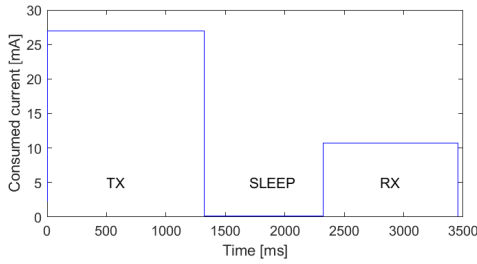


Fig. 3. Current consumption profile for a single LoRaWAN transaction. TX - data transmission state, SLEEP - waiting for reception window, RX - data reception state.

of a single LoRaWAN transaction (here in DR0 mode). The transaction is modeled for all modes as several steps, each described in Table VII.

TABLE VI  
LORAWAN RELATED PARAMETERS

Parameter	Symbol	Value
Preamble length	$L_{preamble}$	8 bits
Uplink payload size	$L_{up}$	128 bits
Ack payload size	$L_{ack}$	128 bits

TABLE VII  
DESCRIPTION OF STEPS IN THE CURRENT CONSUMPTION PROFILE FOR LORAWAN [15]

Step	Time [ms]	Current [mA]
Wake up	1.77	2.27
Packet transmission	$T_{TX}$	27
TX switch off	0.3	2.07
Waiting for reception in sleep	1000	0.12
Packet reception	$T_{RX}$	10.7
RX switch off	0.3	2.05

The transmission time  $T_{TX}$  can be expressed as [34]:

$$T_{TX} = T_{preamble} + T_{uplinkp} \quad (3)$$

and similarly the reception time  $T_{RX}$  becomes:

$$T_{RX} = T_{preamble} + T_{downlinkp} \quad (4)$$

Given parameters from VI, the preamble duration time is expressed as:

$$T_{preamble} = (L_{preamble} + 4.25)T_{sym} \quad (5)$$

where the symbol time is equal to:

$$T_{sym} = \frac{2^{SF}}{BW} \quad (6)$$

with  $BW = 125kHz$ . The uplink payload length is expressed as:

$$L_{uplinkp} = 8 + \max\left(\text{ceil}\left(\frac{L_{up} - 4SF + 44}{4(SF - 2DE)}\right)(CR+4), 0\right) \quad (7)$$

where:

- SF is the spreading factor given in Table II,
- DE is 1 when the low data rate optimization is enabled (DR0, DR1) and 0 when disabled (DR2..5),
- CR is 1 meaning that the coding rate is 4/5.

To calculate downlink ACK payload length  $L_{downlinkp}$ , we substitute  $L_{down}$  instead of  $L_{up}$  in (7). This finally allows us to calculate the duration of the uplink payload  $T_{uplinkp}$ :

$$T_{uplinkp} = L_{uplinkp} \cdot T_{sym} \quad (8)$$

and the duration of the downlink payload  $T_{downlinkp}$ :

$$T_{downlinkp} = L_{downlinkp} \cdot T_{sym} \quad (9)$$

### C. Sigfox transaction

Fig. 4 presents the current consumption profile of a single Sigfox transaction (here using 100 bit/s datarate with downlink packet present). In Sigfox, the uplink data packet is sent 3 times to improve robustness. Each uplink message contains up to 12 bytes of application data and can set a downlink request flag. If set, the device awaits a downlink message from the base station in a reception window of up to 25 s. If downlink message is received, the device transmits a confirmation packet. The transaction is modeled as several steps, each described in Table IX.

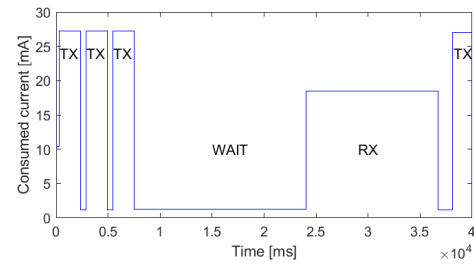


Fig. 4. Current consumption profile for a single Sigfox transaction. TX - data transmission state, RX - data reception state, WAIT - idle state.

TABLE VIII  
SIGFOX RELATED PARAMETERS [17]

Parameter	Symbol	Value
Bit rate	$R$	100 bit/s
Uplink payload size	$L_{up}$	96 bits
Average downlink listening time	$T_{RXAVG}$	12.69 s

The packet transmission time  $T_{TX}$  is expressed as:

$$T_{TX} = \frac{L_{up}}{R} \quad (10)$$

### D. NB-IoT transaction

Bit-exact modeling of an NB-IoT transaction is far more complex than in the case of other analysed protocols, as it involves many processes and mechanisms controlled by various application and operator-related settings. Such modeling has been presented by Sørensen et al. [22] and we will use it to estimate the charge related to a single transaction. To do that

TABLE IX  
DESCRIPTION OF STEPS IN THE CURRENT CONSUMPTION  
PROFILE FOR SIGFOX [17]

Step	Time [ms]	Current [mA]
Wake up	287	10.4
1st packet transmission	$T_{TX}$	27.2
Wait	486	1.2
2nd packet transmission	$T_{TX}$	27.2
Wait	486	1.2
3rd packet transmission	$T_{TX}$	27.2
Waiting for reception window <sup>1</sup>	16493	1.2
Data reception <sup>1</sup>	$T_{RXAVG}$	18.5
Delay before confirmation <sup>1</sup>	1430	1.2
Confirmation transmission <sup>1</sup>	1850	27.2
Switch off	5	1.2

<sup>1</sup> occurs only if the device requested downlink transmission. Otherwise the device switches off after 3rd packet.

we will assume that the transaction will only use PSM mode with minimal time of iDRX and no eDRX and consists of the following phases:

- Synchronization, in which the device operation aligns with the network schedule.
- Service request, assuming the device was previously attached (registered), which sets up the connection.
- Transmission of uplink data and reception of downlink data.
- Connection release.

We will also assume that the PSM sleep mode interval is longer than the actual uplink transmission interval, so that the TAU (Tracking Area Update) messages are not needed.

Given the above assumptions, from [22] Fig.6 we get that:

- For MCS = 2 (Modulation and Coding Scheme) with 8 repetitions the estimated energy per single transaction is approx. 2950 mJ.
- For MCS = 10 with 1 repetition the estimated energy per single transaction is approx. 1530 mJ.

### E. Actislink transaction

Fig. 5 presents the current consumption profile of a single Actislink transaction (here using 0/2 PHY mode).

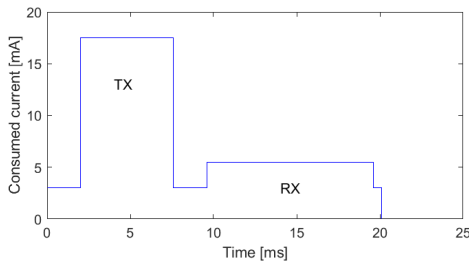


Fig. 5. Current consumption profile for a single Actislink transaction (PHY mode 0/2). TX - data transmission state, RX - data reception state.

TABLE X  
DESCRIPTION OF STEPS IN THE CURRENT CONSUMPTION PROFILE FOR  
ACTISLINK

Step	Time [ms]	Current [mA]
Wake up	2	3
Packet transmission	$T_{TX}$	17.5
Switch to reception	2	3
Confirmation reception	$T_{RXACK}$	5.5
Switch off	0.5	3

TABLE XI  
ACTISLINK PROTOCOL RELATED PARAMETERS

Parameter	Symbol	Value
Uplink payload overhead	$L_{ovh}$	152 bits
Uplink payload size	$L_{up}$	128 bits
Ack packet length	$L_{ack}$	192 bits

Given the values from Table XI the packet transmission time  $T_{TX}$  for a given PHY mode is expressed as:

$$T_{TX} = \frac{L_{ovh} + L_{up}}{R_{up}} \quad (11)$$

where  $R_{up}$  is the uplink bitrate given in Table III. The confirmation reception time  $T_{RXACK}$  can be calculated as:

$$T_{RXACK} = \frac{L_{ack}}{R_{down}} \quad (12)$$

### F. Comparison

Fig. 6 presents the comparison of charge required for a single transaction in all of the analyzed protocols and modes.

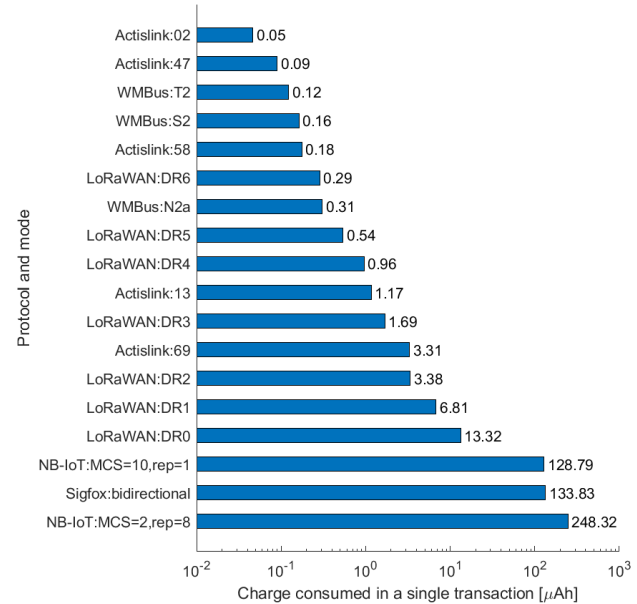


Fig. 6. Comparison of the total charge consumed by a single network transaction in all studied protocols and modes.

## VII. ANALYSIS OF MAXIMUM COUPLING LOSS

Comparing effective range and coverage of each of the presented protocols is difficult, as it relies on many external factors such as terrain and architecture, antenna height and gains etc. It is thus more informative to compare the Maximum Coupling Loss (MCL) allowed in each of the modes of the analyzed protocols. To do that we've gathered a set of transceiver and protocol-related parameters in Table XII, that include sensitivity of the transceiver in given mode and considered output power. The MCL is the difference between the two. Fig. 7 then presents the resulting values of MCL with relation to the charge consumption established in Chapter VI.

TABLE XII  
MCL COMPARISON FOR WIRELESS PROTOCOLS

Protocol	Mode	TX power of meter [dBm]	Base station sensitivity [dBm]	MCL [dB]
WMBus	S2	10	-110 <sup>1,a</sup>	120
	T2	10	-110 <sup>1,a</sup>	120
	N2a	10	-115 <sup>1,a</sup>	125
LoRaWAN	DR0	10	-138 <sup>1</sup>	148
	DR1	10	-134 <sup>1,a</sup>	144
	DR2	10	-131.5 <sup>1,a</sup>	141.5
	DR3	10	-129 <sup>1,a</sup>	139
	DR4	10	-126.5 <sup>1,a</sup>	136.5
	DR5	10	-125 <sup>1</sup>	135
	DR6	10	-122 <sup>1</sup>	132
Sigfox	bidir.	14.5	-132 <sup>2</sup>	146.5
NB-IoT	MCS=10, rep=1	23	-117 <sup>3</sup>	140
	MCS=2, rep=8	23	-127 <sup>3</sup>	150
Actislink	02	12	118 <sup>4</sup>	130
	13	12	135 <sup>4</sup>	147
	47	12	123 <sup>4</sup>	135
	58	12	126 <sup>4</sup>	138
	69	12	140 <sup>4</sup>	154

<sup>1</sup> based on [33] <sup>2</sup> based on [35] <sup>3</sup> Based on [22] <sup>4</sup> based on [31] <sup>a</sup> value approximated based on available documentation

## VIII. COST ANALYSIS

While it is difficult to provide exact cost figure related to the usage of each communication protocol, we can give some general remarks on the following most significant cost components.

### A. Chip cost inside water meter

In general the water meter requires an MCU running the water meter application (and in most cases also the communication protocol) and a radio transceiver. In recent years these two are often integrated withing a single silicon chip. The cost of the chip will most often scale with the amount of RAM and FLASH memory, CPU capabilities and radio capabilities. Table XIII reflects the requirements of the analyzed protocols in that regard.

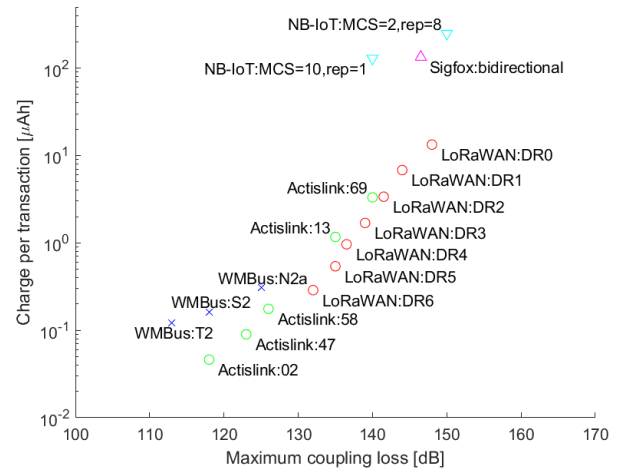


Fig. 7. Charge consumed per single transaction vs maximum coupling loss for the compared protocols and modes.

TABLE XIII  
FACTORS AFFECTING CHIP COST IN A WATER METER

Protocol	RAM footprint	FLASH footprint	Radio capabilities	Overall cost
Wireless M-Bus	low	low	low	low
Actislink	low	medium	low	low
LoRaWAN	low	medium	medium	medium
Sigfox	low	medium	medium	medium
NB-IoT	high	high	high	high

### B. Base station cost and subscription fees

In case of Wireless-MBus, Actislink and LoRaWAN, it is usually up to the user to set up, deploy and manage the infrastructure of base stations. These can vary in price significantly due to their capabilities, build quality, intended operating environment etc. In general, however, the Wireless-MBus base stations will be offered at the lower cost than LoRaWAN and Actislink solutions. In contrary, the subscription fees are related to Sigfox and NB-IoT, as the business model behind these solutions introduces a telecommunications operator.

## IX. CONCLUSIONS

In this article we've analyzed two key aspects of the wireless data transmission protocols used in residential water metering systems - the energy consumption affecting the battery lifetime and maximum coupling loss affecting the range and coverage. In the comparison we've included several major protocols used currently in water meters as well as a newly developed custom protocol (Actislink) designed exclusively for this application. From the gathered results we can conclude, that the communication protocol applied to water meters must be chosen carefully based on the trade off between energy consumption, expected coverage, functionality and cost.

While being the oldest standard, it is not unexpected that Wireless M-Bus performance is worst out of all analyzed protocols. It provides low MCL with relatively high energy



consumption and offers no link adaptation mechanisms. However it comes at the lowest cost for the meter and for the base station.

LoRaWAN offers much better ratio of MCL to energy consumption, and provides good link adaptation mechanisms, but comes at a higher price both for the meter and the base station. This however may be relaxed in the future, as the protocol becomes increasingly popular in many IoT applications.

Sigfox provides no link adaptation mechanism, and has the most stringent limitations on responsiveness. It also yields surprisingly poor relation of MCL to energy, but due to high absolute value of MCL it provides good coverage. It also requires operator fees and is not available in all regions.

Due to the synchronous principle of operation, NB-IoT requires significant amounts of energy and sophisticated hardware, which highly increases the cost of the meter. It seems that in residential water metering applications these can only be compensated by rich functionality and ease of integration with the telecommunication infrastructure.

The Actislink protocol can be considered as a modern evolution of the Wireless M-Bus, offering similar meter cost, but much better ratio of energy consumption to MCL, similar to LoRaWAN. It also offers link adaptation mechanisms, while still relying on relatively low complexity hardware and FSK modulation found in many radio transceivers. It can be considered as a direct replacement of Wireless M-Bus in existing installations, especially in cases where the old standard already proved to be sufficient in terms of coverage.

#### REFERENCES

- [1] Ł. Krzak, M. Kubaszek, J. Macheta, and C. Worek, "Comparison of wireless data transmission protocols for residential water meter applications - Matlab scripts," 2023. [Online]. Available: <https://github.com/lkrzak/ijet2023>
- [2] S. K. Wong and M. Moghavvemi, "A reliable and economically feasible automatic meter reading system using power line distribution network (technical note)," *International Journal of Engineering*, vol. 18, no. 3, pp. 301–318, 2005. [Online]. Available: [https://www.ije.ir/article\\_71596.html](https://www.ije.ir/article_71596.html)
- [3] T. Boyle, D. Giurco, P. Mukheibir, A. Liu, C. Delaney, S. White, and R. Stewart, "Intelligent metering for urban water: A review," *Water*, vol. 5, pp. 1052–1081, 09 2013. [Online]. Available: <https://doi.org/10.3390/w5031052>
- [4] Berg Insight, "Smart water metering in europe and north america. 2nd edition," 2022. [Online]. Available: <https://www.berginsight.com/smart-water-metering-in-europe-and-north-america>
- [5] K. Mekki, E. Bajic, F. Chaxel, and F. Meyer, "A comparative study of lpwan technologies for large-scale iot deployment," *ICT Express*, vol. 5, no. 1, pp. 1–7, 2019. [Online]. Available: <https://doi.org/10.1016/j.ict.2017.12.005>
- [6] P. Levchenko, D. Bankov, E. Khorov, and A. Lyakhov, "Performance comparison of nb-fi, sigfox, and lorawan," *Sensors*, vol. 22, no. 24, 2022. [Online]. Available: <https://doi.org/10.3390/s22249633>
- [7] Y. Lalle, L. C. Fourati, M. Fourati, and J. P. Barraca, "A comparative study of lorawan, sigfox, and nb-iot for smart water grid," in *2019 Global Information Infrastructure and Networking Symposium (GIIS)*, 2019, pp. 1–6. [Online]. Available: <https://doi.org/10.1109/GIIS48668.2019.9044961>
- [8] N. Sushma, H. N. Suresh, J. M. Lakshmi, P. N. Srinivasu, A. K. Bhoi, and P. Barsocchi, "A unified metering system deployed for water and energy monitoring in smart city," *IEEE Access*, vol. 11, pp. 80 429–80 447, 2023. [Online]. Available: <https://doi.org/10.1109/ACCESS.2023.3299825>
- [9] P. Ruckebusch, S. Giannoulis, I. Moerman, J. Hoebeke, and E. De Poorter, "Modelling the energy consumption for over-the-air software updates in lpwan networks: Sigfox, lora and ieee 802.15.4g," *Internet of Things*, vol. 3–4, pp. 104–119, 2018. [Online]. Available: <https://doi.org/10.1016/j.iot.2018.09.010>
- [10] S. M. Phal, G. R. Salanke N.S., S. G., and P. S.B., "Intelligent meters for urban domestic water consumption," in *2019 IEEE International Conference on Cloud Computing in Emerging Markets (CCEM)*, 2019, pp. 59–63. [Online]. Available: <https://doi.org/10.1109/CCEM48484.2019.00013>
- [11] F. Abate, M. Carratù, C. Liguori, and V. Paciello, "A low cost smart power meter for iot," *Measurement*, vol. 136, pp. 59–66, 2019. [Online]. Available: <https://doi.org/10.1016/j.measurement.2018.12.069>
- [12] S. Spinsante, S. Squartini, L. Gabrielli, M. Pizzichini, E. Gambi, and F. Piazza, "Wireless m-bus sensor networks for smart water grids: Analysis and results," *International Journal of Distributed Sensor Networks*, vol. 10, no. 6, p. 579271, 2014. [Online]. Available: <https://doi.org/10.1155/2014/579271>
- [13] S. Squartini, L. Gabrielli, M. Mencarelli, M. Pizzichini, S. Spinsante, and F. Piazza, "Wireless m-bus sensor nodes in smart water grids: The energy issue," in *2013 Fourth International Conference on Intelligent Control and Information Processing (ICICIP)*, 2013, pp. 614–619. [Online]. Available: <https://doi.org/10.1109/ICICIP.2013.6568148>
- [14] L. Casals Ibáñez, B. Mir Masnou, R. Vidal Ferré, and C. Gomez, "Modeling the energy performance of lorawan," *Sensors*, vol. 17, p. 2364, 10 2017. [Online]. Available: <https://doi.org/10.3390/s17102364>
- [15] S. Maudet, G. Andrieux, R. Chevillon, and J.-F. Diouris, "Refined node energy consumption modeling in a lorawan network," *Sensors*, vol. 21, no. 19, p. 6398, Sep 2021. [Online]. Available: <http://doi.org/10.3390/s21196398>
- [16] S. Trendov, M. Gering, and E. Siemens, "Impact of lorawan transceiver on end device battery lifetime," in *2023 30th International Conference on Systems, Signals and Image Processing (IWSSIP)*, 2023, pp. 1–5. [Online]. Available: <https://doi.org/10.1109/IWSSIP58668.2023.10180293>
- [17] C. Gomez, J. Veras, R. Vidal Ferré, L. Casals Ibáñez, and J. Paradells, "A sigfox energy consumption model," *Sensors*, vol. 19, p. 681, 02 2019. [Online]. Available: <https://doi.org/10.3390/s19030681>
- [18] M. Naeem, M. Albano, K. G. Larsen, B. Nielsen, A. Høedholt, and C. Ø. Laursen, "Modelling and analysis of a sigfox-based iot network using uppaalsmc," *IEEE Sensors Journal*, vol. 23, no. 10, pp. 10 577–10 587, 2023. [Online]. Available: <https://doi.org/10.1109/JSEN.2023.3261667>
- [19] A. K. Sultania, P. Zand, C. Blondia, and J. Famaey, "Energy modeling and evaluation of nb-iot with psm and edrx," in *2018 IEEE Globecom Workshops (GC Wkshps)*, 2018, pp. 1–7. [Online]. Available: <https://doi.org/10.1109/GLOCOMW.2018.8644074>
- [20] C. B. Mwakwata, H. Malik, M. Mahtab Alam, Y. Le Moullec, S. Parand, and S. Mumtaz, "Narrowband internet of things (nb-iot): From physical (phy) and media access control (mac) layers perspectives," *Sensors*, vol. 19, no. 11, 2019. [Online]. Available: <https://doi.org/10.3390/s19112613>
- [21] M. Lukic, S. Sobot, I. Mezei, D. Vukobratovic, and D. Danilovic, "In-depth real-world evaluation of nb-iot module energy consumption," in *2020 IEEE International Conference on Smart Internet of Things (SmartIoT)*, 2020, pp. 261–265. [Online]. Available: <https://doi.org/10.1109/SmartIoT49966.2020.00046>
- [22] A. Sorensen, H. Wang, M. J. Remy, N. Kjettrup, R. B. Sorensen, J. J. Nielsen, P. Popovski, and G. C. Madueno, "Modeling and experimental validation for battery lifetime estimation in NB-IoT and LTE-m," *IEEE Internet of Things Journal*, vol. 9, no. 12, pp. 9804–9819, jun 2022. [Online]. Available: <https://doi.org/10.1109/jiot.2022.3152173>
- [23] European Standard, "EN 13757-4:2019 - Communication systems for meters and remote reading of meters - Part 4: Wireless meter readout (Radio meter reading for operation in SRD bands)," 2019.
- [24] LoRa Alliance, "Lorawan® regional parameters rp002-1.0.4," 2022. [Online]. Available: <https://resources.lora-alliance.org/technical-specifications/rp002-1-0-4-regional-parameters>
- [25] SIGFOX, "Sigfox technical overview," May 2017. [Online]. Available: <https://api.build.sigfox.com/files/59c211c69d14790001fbc9a2>
- [26] S. Aguilar, A. Platis, R. Vidal, and C. Gomez, "Energy consumption model of schc packet fragmentation over sigfox lpwan," *Sensors*, vol. 22, no. 6, 2022. [Online]. Available: <https://doi.org/10.3390/s22062120>
- [27] P. Thubert, "An Architecture for IPv6 over the Time-Slotted Channel Hopping Mode of IEEE 802.15.4 (6TiSCH)," RFC 9030, May 2021. [Online]. Available: <https://www.rfc-editor.org/info/rfc9030>
- [28] M. Kubaszek, J. Macheta, Ł. Krzak, and C. Worek, "The analysis of energy consumption in 6tisch network nodes working in sub-ghz band," *International Journal of Electronics and Telecommunications*, vol. vol. 66, no. No 1, pp. 201–210, 2020. [Online]. Available: <https://doi.org/10.24425/ijet.2020.131864>

- [29] M. R. S. Jagir Hussain, "Be-rpl: Balanced-load and energy-efficient rpl," *Computer Systems Science and Engineering*, vol. 45, no. 1, pp. 785–801, 2023. [Online]. Available: <http://doi.org/10.32604/csse.2023.030393>
- [30] I. F. V. Junior, J. Granjal, and M. Curado, "A distributed network-aware tsch scheduling," in *2023 19th International Conference on the Design of Reliable Communication Networks (DRCN)*, 2023, pp. 1–8. [Online]. Available: <https://doi.org/10.1109/DRCN57075.2023.10108193>
- [31] Ł. Krzak, C. Worek, G. Gajoch, and J. Witkowski, "Adaptive radio communication layer for a stationary water meter reading system," *Przegląd Elektrotechniczny*, 2022. [Online]. Available: <https://doi.org/10.15199/48.2022.01.24>
- [32] C. Worek, Ł. Krzak, G. Gajoch, and J. Witkowski, "Two-band, sdr-based base station for smart metering applications," *Przegląd Elektrotechniczny*, 2022. [Online]. Available: <https://doi.org/10.15199/48.2022.01.26>
- [33] ST Microelectronics, "Datasheet of stm32wle5xx and stm32wle4xx (ds13105 rev 12)," 2022.
- [34] Semtech, "Sx1272/3/6/7/8 lora modem design guide," 2013.
- [35] SIGFOX, "Sigfox access station micro smbs-t4 datasheet," 2023. [Online]. Available: <https://support.sigfox.com/docs/smbs-t4-datasheet>